

Original scientific paper  
UDC 551.511.61

## Refinement of the vertical diffusion scheme in the ARPÈGE/ALADIN model

Maja Telišman Prtenjak<sup>1</sup>, Antun Marki<sup>1</sup> and Pierre Bénard<sup>2</sup>

<sup>1</sup>Andrija Mohorovičić Geophysical Institute, Faculty of Science,  
University of Zagreb, Zagreb, Croatia

<sup>2</sup>Centre National de Recherches Météorologiques, Groupe de Modélisation pour  
l'Assimilation et la Prévision, Toulouse Cedex, France

Received 24 September 1998, in final form 26 March 1999

In atmospheric numerical weather prediction (NWP) models, the use of long time-steps as allowed by efficient numerical/dynamical schemes can lead to spurious oscillations due to the parameterized physical part. Typical examples of this are the oscillations associated with simplified parameterization schemes for vertical diffusion or shallow-convection, such as usually used for NWP.

The oscillations generated by *K*-type vertical-diffusion schemes are well documented, and being called *fibrillations*; they are characterized by high temporal and vertical frequencies. Since they are linked to high vertical resolution, these spurious oscillations are generally found in the low-levels of model's domain.

In ARPÈGE, the MÉTÉO-FRANCE NWP global model, and in ALADIN, its limited-area model (LAM) version developed in cooperation with Eastern European countries, and also used for operational NWP purpose, some oscillations still remained in the evolution of the forecast fields, despite the fact that a first anti-fibrillation scheme (AFS) had been included. This study was made to examine the possible sources of these oscillations, through the 1-D (vertical) version of these models.

First, the parameterization of shallow-convection (which is in fact part of the vertical diffusion scheme) was found to be an important source of oscillations, and some solutions for eliminating this problem are proposed. Second, the original AFS is shown not to completely prevent the generation of fibrillations, and a more efficient formulation is derived.

All AFSs basically consist in a temporal first-order decentering of the diffusion equation, keeping an explicit form for the exchange coefficient itself. The AFS correction thus always improves the stability at the expense of the accuracy in some way. In the new AFS proposed here, the number of grid-points which need a correction is lessened from almost 90% to some 5%, resulting in a more accurate scheme. Unlike AFSs proposed in the literature, the correction has now to be applied not only for grid points of atmospheric stable conditions (*i.e.* Richardson number,  $Ri > 0$ ) but also for atmospheric slightly unstable conditions ( $Ri < 0$ ).

**Keywords:** NWP model, ARPÈGE/ALADIN model, shallow-convection, Richardson number, fibrillation, anti-fibrillation scheme.

## 1. Introduction

Numerical Weather Prediction (NWP) models are now using numerical/dynamical schemes far more efficient than in the past. For instance, the use of a two-time-level semi-Lagrangian scheme commonly allows an increase of the time-step by a factor 6 for typical NWP applications, compared to a classical Eulerian leap-frog semi-implicit scheme. Part of this time-step increase is however not transparent from the physical parameterizations point of view, and schemes which were satisfactorily behaving for moderate time-steps now exhibit undesired instabilities in some cases.

A well documented example (Kalnay and Kanamitsu, 1988; Girard and Delage, 1990) of this kind of instability appears when using non-linear vertical diffusion schemes based on an exchange coefficient formulation (traditionally called K-type vertical diffusion schemes). In these schemes, the non-linear vertical diffusion for any prognostic variable  $\psi$  is represented by:

$$\frac{\partial \psi}{\partial t} = \frac{\partial}{\partial z} \left( K_{\psi} \frac{\partial \psi}{\partial z} \right)$$

where  $K_{\psi}$ , the turbulent exchange coefficient of the variable  $\psi$ , is somehow a function of the Richardson number  $Ri$ , thus computed diagnostically from the flow.

For insuring the stability of the parameterization, an implicit backward scheme for the variable  $\psi$  is used, but the coefficient  $K_{\psi}$  has to be kept explicit for the feasibility of the computations. Kalnay and Kanamitsu (1988) analyzed general characteristics of various numerical schemes on strong non-linear damping equations. They showed that this system has a much wider range of non-linear stability than a fully explicit scheme but that it can also become linearly unstable. The non-linear solution is then oscillating around the correct value, the magnitude of the oscillations remaining bounded, due to non-linear effects. This kind of spurious oscillations is hereafter called *fibrillations*. To prevent linear instability of this kind, Girard and Delage (1990) (hereafter GD90) developed an anti-fibrillation scheme (AFS) for the NWP model of the Canadian Meteorological Center. The principle of GD90's AFS is to apply a temporal decentering factor  $\beta$  to the time-discretized diffusion equation:

$$\frac{\partial \psi}{\partial t} = \frac{\partial}{\partial z} \left[ (1 - \beta) \left( K_{\psi} \frac{\partial \psi}{\partial z} \right) + \beta \left( K_{\psi} \frac{\partial \psi^+}{\partial z} \right) \right]$$

where  $\psi^+$  denotes  $\psi$  at the future physics time-step. Note that the decentering factor is applied not to the physical tendencies, but to the fluxes themselves, thus allowing a conservative form of the scheme even in the case of a

vertical variation of  $\beta$ . The value  $\beta = 1$  gives the normal implicit diffusion scheme (without AFS), while specifying  $\beta > 1$  large enough leads to a stable scheme. However, the above decentering is only first-order accurate in time, and cannot be used without distorting the solution. The key idea of GD90 is thus to make  $\beta$  flow-dependent to achieve a minimal correction, sufficient to insure stability, but weak enough not to lead to significant distortion. They consider the variations of  $K$  during the time step by calculating its derivative with respect to the basic variables. Numerical analysis of the set of two coupled diffusion equations for zonal ( $u$ ) wind component and potential temperature ( $\Theta$ ) is made to illustrate the main features of the nonlinear instability problem. They find that stability of numerical solutions requires

$$1 + \gamma_{\max} K \left( \beta - 1 + \frac{\alpha}{2} \right) \geq 0 \quad (1)$$

where

$$\gamma_{\max} = \frac{4\Delta t}{(\Delta z)^2}$$

$$\alpha = \frac{nb|Ri|}{1 - b|Ri|}$$

In Eq. (1),  $\gamma_{\max}$  is a discretization factor dependent on vertical increment ( $\Delta z$ ) and time-step ( $\Delta t$ ),  $n$  and  $b$  are parameters used to define the dependency of  $K$  with respect to  $Ri$ . The crucial point is that in GD90, this dependency is assumed to be the same for dynamical and thermal exchange coefficients, to simplify the computations. The above stability condition implies that for  $\beta = 1$ , linear numerical instability will occur only if  $\alpha < 0$ , a condition which is equivalent to atmospheric stable conditions ( $Ri > 0$ ) since  $n$  and  $Ri$  have opposite signs. They proposed that oscillatory solutions could be prevented with the following condition:

$$\beta = \max \left[ \left( 1 - \frac{\alpha}{2} \right), \left( 2 - \alpha \right) - \frac{1}{\gamma_{\max} K} \right]$$

Slightly modified AFS scheme based on the same analysis has been implemented in ARPÈGE, the global NWP model (Courtier *et al.*, 1991), and its LAM version ALADIN (*e.g.*: Bubnová *et al.*, 1993; ALADIN International Team, 1997), and will be studied later.

Another oscillation problem may arise with long time-steps when using simple parameterizations of the shallow convection. For the computation of vertical exchange coefficients  $K$ , existence of shallow convective clouds at the top of the Atmospheric Boundary Layer (ABL) is very important. In that

case, standard »dry-computed«  $K$ -approach for expressing the turbulence in the ABL does not give satisfactory results: the moisture turbulent fluxes remain confined to the ABL and the moisture flux toward the free atmosphere is not sufficient, resulting in an insulated moist ABL. To solve this problem, a parameterization of the vertical exchange in the ABL in the presence of shallow convection has been developed in ARPÈGE and ALADIN, following Geleyn (1987), by computing vertical exchange coefficients  $K$  with a modified Richardson number which takes into account the moisture profile in the ABL. The shallow-convection is thus parameterized as a correction of the vertical diffusion scheme, acting in the sense to allow an upward diffusion of moisture in case of a saturated ABL.

When increasing the time-step as allowed by the switch to a semi-Lagrangian transport scheme in ARPÈGE/ALADIN, it was found that temporal oscillations appeared in the predicted meteorological variables, due to the original physical parameterization package. This study analyses the weaknesses of this original package regarding to long time-steps, and proposes some solutions for stabilizing the involved schemes. In the section 2, the relevant features for the present state of ARPÈGE/ALADIN are described. This description includes the two involved parameterizations schemes (AFS and shallow convection correction) as well as the settings used for the numerical experiments discussed hereafter. The remaining of the paper is divided into two parts: in the first part, the role of the shallow-convection correction is examined. It is shown that oscillations that are caused by this correction are not fibrillations in the above-mentioned sense, and appropriate treatments are proposed to eliminate the oscillatory behavior (Section 3). In the second part, the existence of residual fibrillations in spite of the original AFS application is demonstrated, and a new solution for eliminating these fibrillations is presented (Section 4). Section 5 contains a summary.

## 2. The ARPÈGE/ALADIN model

### 2.1. Vertical coordinate

In ARPÈGE/ALADIN, the vertical spacing of the hybrid terrain-following pressure-type coordinate ( $\eta$ ) levels is variable as done classically to allow a finer description of the surface processes. However, the finer vertical resolution near the surface can become a potential source of numerical problems: temporal oscillations in the forecast fields can be occasionally observed in the lowest levels of the domain though the time-step was chosen in order to avoid most of these oscillations. We were able to reproduce these oscillations in the 1-D single column version of ARPÈGE/ALADIN model and thus they will be studied here in the framework of this 1-D model to allow a better identifica-

tion of the process. In this 1-D model, the physics package, and the vertical discretization are exactly identical as in the 3-D model (Simmons and Burridge, 1981). The atmosphere depth is divided into  $l$  layers (and  $l + 1$  interfaces between these layers). The vertical discretisation only defines the position of the interfaces, where fluxes and advective vertical velocities are defined. The other (prognostic) variables of the model are defined in a staggered manner, at a level representative of the layer (usually half-way of interfaces in terms of  $\eta$ , but other options are possible). The vertical discretisation scheme is based on a vertically staggered grid. Fluxes and advecting vertical velocities are defined at layer interfaces, while model variables are defined at model levels representative of each layer. The first layer interface is at zero pressure and the last one is at the surface. The main notations and grid organization are shown in Figure 1. A variable at level is denoted as  $Q_l$ . A variable at the interface between level  $l$  above and level  $l + 1$  below is denoted as  $Q_i$ .

2.2. Modified Richardson number for shallow convection representation ( $Ri^*$ )

When the vertical gradient of dry static energy increases, the definition of  $Ri$  implies an inhibition of vertical exchanges. This can lead to a large under-estimation of moisture fluxes arising in case of shallow convection at the top of the ABL (an important feature in tropical areas for the moisture

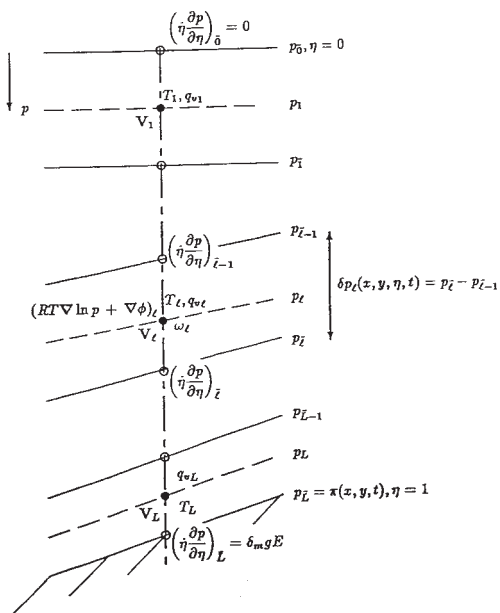


Figure 1. Vertical discretisation of ARPEGE/ALADIN model.

budget). To take into account the impact of shallow convection on the budget of the atmosphere, a modified Richardson number  $Ri^*$  is included in ARPÈGE/ALADIN and used for the computation of the exchange coefficients, instead of the classical form of the Richardson number.  $Ri^*$  is defined as follows (Geleyn, 1987):

$$Ri^* = \frac{g}{C_p T} \frac{\frac{\partial s}{\partial z} + L \min\left(0, \frac{\partial q}{\partial z} - \frac{\partial q_s}{\partial z}\right) \delta^h}{\left\| \frac{\partial \mathbf{V}}{\partial z} \right\|} \quad (2)$$

where:

$g$  – acceleration of gravity (m/s<sup>2</sup>);

$T$  – temperature (K);

$C_p$  – specific heat at constant pressure (J/kgK);

$z$  – vertical coordinate (m);

$s = C_p T + gz$  – dry static energy (J/kg);

$L$  – latent heat (J/kg);

$q$  – specific humidity (g/kg);

$\mathbf{V}$  – wind velocity (m/s);

$\delta^h$  – Kronecker symbol for limiting the scheme to conditionally unstable layers when leaving the ABL;

$q_s$  – saturation specific humidity (g/kg).

Since this shallow convection instability triggers when the humidity profile reaches the saturated one, the corrective term in  $Ri^*$  then allows an increase of vertical exchanges in this case. This modified Richardson number is then used to compute the exchange coefficients in place of the normal one  $Ri$ . The second term in the numerator of Eq. (2) will be referred to as correction for shallow convection (CSC) hereafter. Since it is always negative, it always reduces the stability of the flow thus increasing vertical exchanges when the humidity profile reaches the saturated one. The  $\delta^h$  multiplier is added to prevent activation of the correction in undesired layers of the domain (*e.g.* in the stratosphere).

### 2.3. Anti-fibrillation scheme

Unlike in GD90, the exchange dynamical and thermal exchange coefficients  $K_u$  and  $K_\theta$  have a distinct expression in ARPÈGE/ALADIN and in most NWP models defined as follows (Courtier et al., 1991):

$$K_u = l^2 \left| \frac{\partial u}{\partial z} \right| f_u(Ri) \quad (3)$$

$$K_{\Theta} = l^2 \left| \frac{\partial u}{\partial z} \right| f_{\Theta}(Ri) \quad (4)$$

where  $l$  is mixing length (kept constant here) and  $f_u(Ri)$  and  $f_{\Theta}(Ri)$  are functions of the Richardson number ( $Ri$ ), defined by:

$$Ri = \frac{g}{\Theta_0} \frac{\Theta_z}{(u_z)^2}. \quad (5)$$

The coupled system of equations for perturbations of zonal wind  $u$  and sensible heat flux represented by potential temperature  $\Theta$  is taken. The original ARPÈGE/ALADIN diffusion equations are (Courtier *et al.*, 1991):

$$\frac{\partial \Theta}{\partial t} = \frac{\partial}{\partial z} \left( K_{\Theta} \frac{\partial \Theta}{\partial z} \right) \quad (6)$$

$$\frac{\partial u}{\partial t} = \frac{\partial}{\partial z} \left( K_u \frac{\partial u}{\partial z} \right) \quad (7)$$

If one performs the stability analysis of this system for a small perturbation (cf. Appendix A), the numerical growth rate  $x = (1 - \tau)$  will be linked to the decentering factor  $\beta$  through the following stability equation:

$$\begin{aligned} &\tau^2[(1 + \beta\gamma K_u)(1 + \beta\gamma K_{\Theta})] + \tau[(1 + \beta\gamma K_u)\gamma K_{\Theta}(1 + \alpha_{\Theta}) + \\ &(1 + \beta\gamma K_{\Theta})\gamma K_u(2 - 2\alpha_u)] + [\gamma^2 K_u K_{\Theta}(2 - 3\alpha_u + 2\alpha_{\Theta})] = 0 \end{aligned} \quad (8)$$

where

$$\alpha_u = \frac{Ri}{f_u} \frac{df_u}{dRi} \quad (9)$$

$$\alpha_{\Theta} = \frac{Ri}{f_{\Theta}} \frac{df_{\Theta}}{dRi} \quad (10)$$

In the original version of ARPÈGE/ALADIN's AFS, it has been assumed that the terms  $\beta\gamma K$  were dominant in (8) (according to large time-steps used) and a simpler equation was then obtained, which was solved by the new variable  $y = \tau\beta$ :

$$y^2 - Sy + P = 0 \quad (11)$$

where:

$$S = -(3 - 2\alpha_u + \alpha_{\Theta})$$

$$P = 2 - 3\alpha_u + 2\alpha_{\Theta}$$

Two negative roots are obtained ( $y_1$  and  $y_2$ ) and the one with maximum absolute value should be chosen ( $|y_{\max}|$ ). Numerical stability is achieved if  $x_{1,2} \geq -1$  and oscillations are completely damped for  $x_{1,2} \geq 0$ , *i.e.*:

$$\text{stability: } \beta \geq -y_{\max}/2$$

$$\text{no oscillation: } \beta \geq -y_{\max}.$$

In the resulting scheme,  $\beta$  is thus locally chosen as:

$$\beta = \max [1, 0.5 \lambda |y_{\max}|]$$

where  $\lambda$  is a free parameter for tuning the magnitude of the correction, with the default value of 1 (which corresponds to stability only). In the following, the complete stability equation (8) is written in a more concise way as:

$$F(\beta, \tau) = \tau^2 A(\beta) + \tau B(\beta) + C(\beta) = 0 \quad (12)$$

#### 2.4. Numerical experiments settings

For the numerical experiments, the initial profiles were taken from 3-D ARPÈGE integrations with evidence of oscillations. For the study of shallow convection instabilities (Section 3), a point located at (41.53 °N, 0.0 °W) was chosen for the 1995/07/02 at 00UTC, the model had 15 levels, and advective terms of prognostic variables were specified from an integration of the 3D version of the model on the same case. For the study of vertical diffusion instabilities (Section 4), the chosen point was (15.53 °N, 140.05 °W) on 1996/09/30 at 00UTC (approximately 15:00 local time). The model had 27 levels and was used in free mode (*i.e.* no dynamical forcing was applied from the 3D model). Of course in every cases the radiative forcing is applied in order to correctly describe the diurnal cycle.

A leap-frog temporal scheme was used for discretising time-differential terms. Integrations were made with different time-steps (in the case of shallow convection  $\Delta t$  was 576 seconds and in the case of AFS,  $\Delta t$  was 200, 400, 600, 981.82 and 1200 seconds). The integration time span was always 24 hours.

All the analytical developments below have been made using a two-time levels marching scheme. However, for leap-frog schemes, all the analyses remain formally unchanged, except that the prognostic variables  $\psi$  (resp.  $\Delta t$ ) becomes  $\psi$  (resp.  $2\Delta t$ ) everywhere, and all the results found for the two-time level schemes apply to each time-decoupled solution of the leap-frog scheme. As a consequence, an instability giving rise to  $2\Delta t$  oscillations in a two-time level scheme, will produce a  $4\Delta t$  oscillation with the leap-frog scheme.



### 3. New parameterization for shallow convection

The temperature and wind components have been found to be the most sensitive variables for the oscillations occurring due to the shallow convection parameterization. But oscillations are not present at all model levels. For instance, temperature time integration at all levels during 24 hours, showed that the highest 8 levels were completely free of oscillations. This is not surprising since the discretisation and all physical schemes are less stringent near the top of the domain.

Our attention was thus focused on level 11, which is located near the top of the ABL. First we made some tests with and without activation of shallow convection calculations: Figure 2a shows the evolution of the temperature with correction for shallow convection (CSC) activated (line 1), and not activated (line 2). Oscillations on the Figure 2a in case of *CSC* activated were a first warning on the possible disadvantage of Eq. (2) in the framework of used anti-fibrillation scheme. In this section, the *CSC* is thus activated all the time.

Temporal oscillations were also found to appear when  $Ri^*$  was replaced with »dry-computed«  $Ri$  for the numerical stability analysis part of the AFS, in such a way that shallow convection then could not influence on possible fibrillations. On Figure 2b are plotted both temperature and *CSC* at the same level. Comparison of these two curves shows that every time-step when *CSC* is non-zero (*i.e.* shallow convection acting); the model produces oscillations except when two successive *CSC* are acting. When *CSC* is acting only once, the solution oscillates, but with a damped magnitude in time. This behavior is indicative of the fact that the real source of oscillations is not the activation of *CSC* by itself but rather the triggering of the computational mode in the temporal scheme ( $2\Delta t$  oscillations) by the intermittence of the *CSC* term. The computational mode is not completely filtered when using a leap-frog scheme, and any intermittent process is able to generate computational oscillatory response. When the *CSC* is acting with a similar magnitude for two successive time-steps, the computational mode is not triggered. The damped magnitude of the oscillations is due to the Asselin time filter (Haltiner and Williams, 1980) which is activated for all leap-frog versions of the ARPÈGE model. Asselin time filter is defined as following:

$$\overline{\psi}_t = \psi_t + a(\overline{\psi}_{t-\Delta t} - 2\psi_t + \psi_{t+\Delta t})$$

where the overlined values correspond to the filtered and the plain values are the yet unfiltered raw results.

This statement can be checked by changing the value of the Asselin filter coefficient  $a$  from the normal value of 0.05 to 0.49. Doing this, the computational mode of the leap-frog scheme is almost completely filtered, at the expense, of course, of the accuracy of the scheme. The expected behavior should

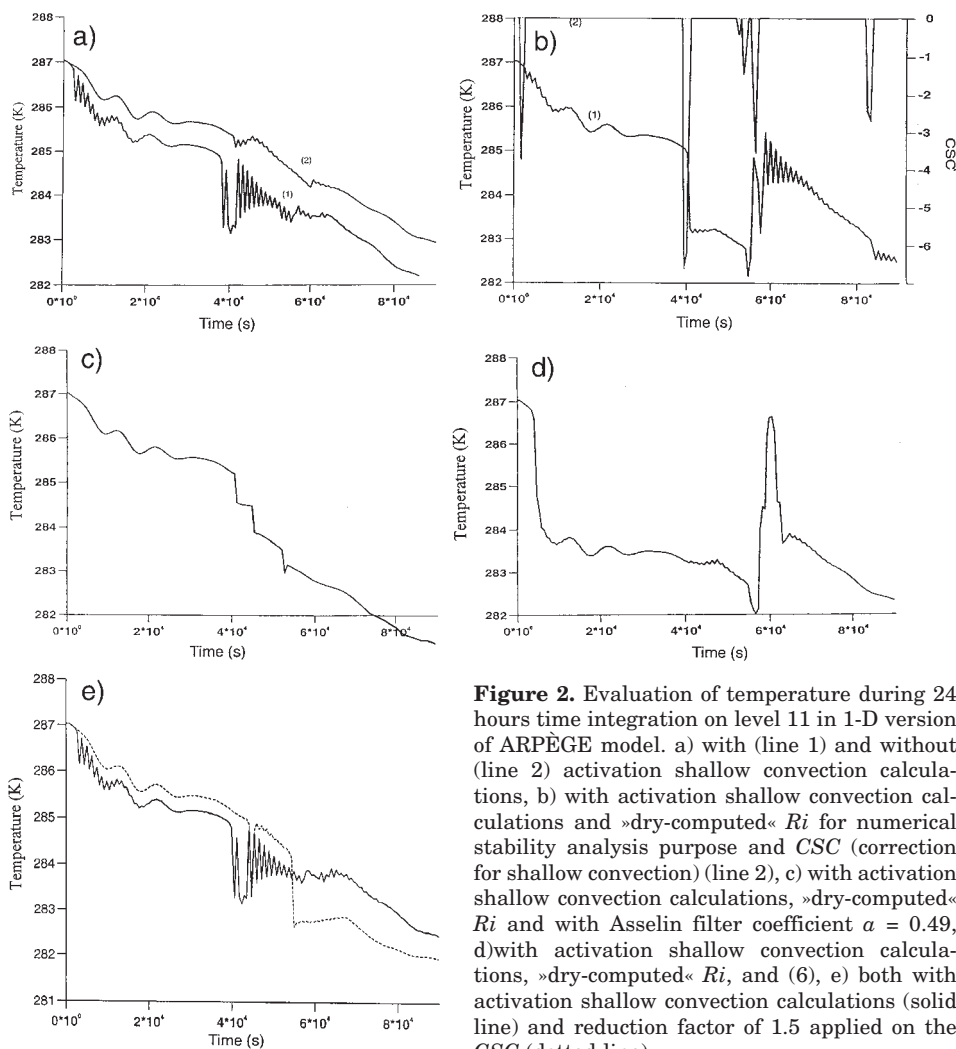


**Figure 2.** Evaluation of temperature during 24 hours time integration on level 11 in 1-D version of ARPÈGE model. a) with (line 1) and without (line 2) activation shallow convection calculations, b) with activation shallow convection calculations and »dry-computed«  $Ri$  for numerical stability analysis purpose and  $CSC$  (correction for shallow convection) (line 2), c) with activation shallow convection calculations, »dry-computed«  $Ri$  and with Asselin filter coefficient  $a = 0.49$ , d) with activation shallow convection calculations, »dry-computed«  $Ri$ , and (6), e) both with activation shallow convection calculations (solid line) and reduction factor of 1.5 applied on the  $CSC$  (dotted line).

then be the disappearance of computational mode oscillations. This is confirmed on Figure 2c, where a significant deviation from the reference experiment can also be observed, due to the loss of accuracy of the scheme.

In order to prevent the intermittent behavior of the  $CSC$ , a new formulation was defined, for which the  $CSC$  is computed as a geometrical series in time:

$$CSC^*(t, z) = \frac{1}{2} [CSC(t, z) + CSC^*(t - \Delta t, z)] \quad (13)$$

where  $CSC^*$  represents the »time-filtered« value and  $CSC$  the instantaneous value of the shallow convection correction.

Such an approach protects the  $CSC$  against intermittence, and decreases the oscillatory response of the model, while attempting to keep the net magnitude of the correction in time. The effect of this modification is shown on Figure 2d: the obtained solution is effectively oscillation-free. The evolution is significantly affected, especially during the first half of the integration, because of the cumulative effect of the different evolution for each neighboring layers (the negative and positive pulses near 60000s can be interpreted as a transient perturbation vertically propagating through the modified vertical diffusion process).

Another way to prevent oscillations due to the  $CSC$  is to decrease its amplitude. This approach implicitly makes the assumption that the adjustment will finally be equivalent, but after a longer time if the correction is smaller. This is of course true only in a small domain around the magnitude of the normal correction, since the process is highly non-linear. For example, a decrease of the  $CSC$  by a factor 5 is very efficient for eliminating oscillations in the prognostic variables, but can be shown to lead to an erroneous vertical structure of the ABL, similarly to the case where  $CSC$  is not activated. Smaller values can however give satisfactory result. Figure 2e shows the evolution of the temperature with a reduction factor of 1.5 applied on the  $CSC$ : the oscillations are removed, and the evolution is globally similar to the normal  $CSC$  case.

Various methods can thus be applied to remove the intermittence of the  $CSC$  in leap-frog and the choice will have to be made on the basis of the validation scores and of the maintenance of a realistic vertical structure for the ABL, also considering the possibility to apply new ideas for this well identified problem.

#### 4. Proposals for the new anti-fibrillation scheme

Once understood the source of oscillations due to the  $CSC$  and some possible solution proposed, the focus was then put on the main other source of oscillations due to the instability of the vertical diffusion scheme in some situations. In this section, the  $CSC$  is not activated, in order to avoid mixing the two possible causes of oscillations in the integrations. According to the past experience, fibrillations in the vertical diffusion scheme are expected for small vertical mesh and long time-steps. The behavior of the operational AFS in 1-D integrations for the studied column of the 3-D domain is shown on Figures 3a, 3b for different time-steps (200, 600, and 1200 s). The obtained evo-

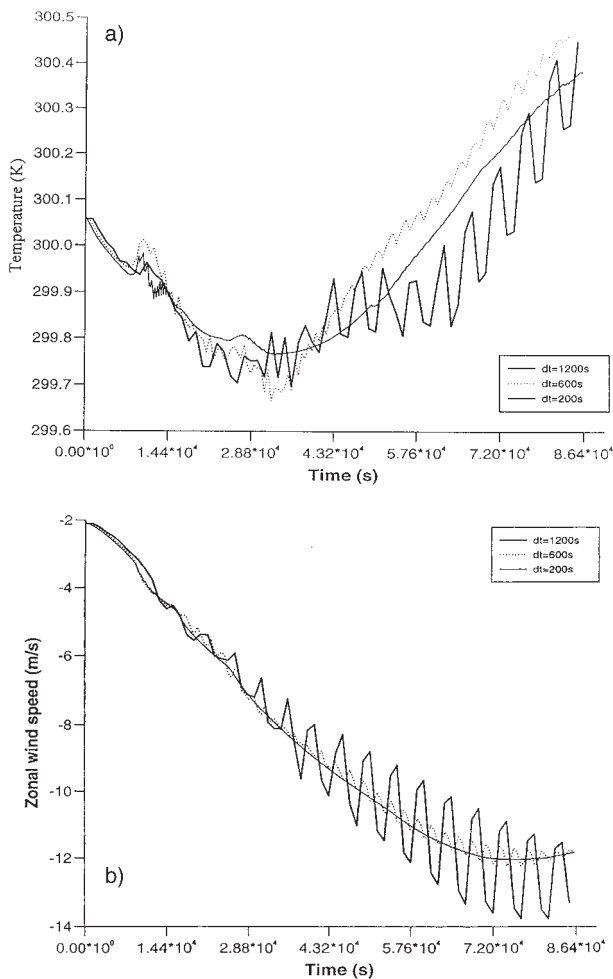


**Figure 3.** Evaluations of a) potential temperature and b) zonal wind component,  $u$  during 24 hours time integration on level 26 in 1-D version of ARPÈGE model (without activation shallow convection calculations and  $\lambda = 1$ ); operational AFS is used for time steps: 200, 600 and 1200s.

lutions for surface temperature and zonal component of the surface wind velocity clearly show an increasing level of noise for time-steps 600s to 1200s as expected from the stability analysis of the fibrillation process. The fibrillations are the oscillations, which exhibit a spurious regular pattern in the second half of the integration. The irregular oscillations near the minimum in Figure 3a for instance should be viewed as the normal response of the flow to the physical parameterizations, which damping is of course not the object of the AFS.

The appearance of fibrillations, although the original (*i.e.* operational) AFS was turned to act, was a sign that this formulation of the AFS was not fully efficient, and that some changes would have to be done through the

specification of the  $\beta$  parameter. Figure 4 shows the dependence of the local correction (decentering) factor  $\beta$  with the Richardson number for all grid points during all the integration, obtained with the operational AFS. One can notice that every point in the stable ( $Ri > 0$ ) region of the atmosphere is corrected (*i.e.*  $\beta > 1$ ), by a factor which can reach 14%. Even for the very stable cases (80% of all the points) the correction was acting. This is not consistent

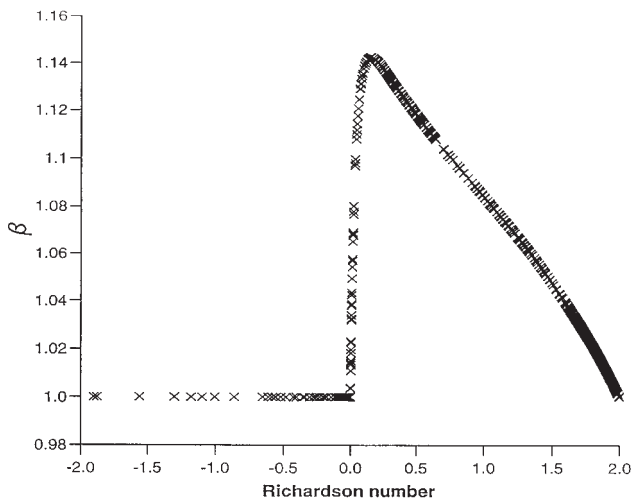


**Figure 4.**  $\beta$  values used by operational AFS (with  $\Delta t = 1200s$ ,  $\lambda = 1$ , without activation shallow convection calculations and correction for reduction of  $Ri \gg 1$  included) versus  $Ri$ . Few grid points with  $Ri < -2$  are omitted.

with the expected behavior since these atmospheric stable points are not likely to generate oscillations. This comes from the fact that for very stable conditions,  $\gamma\beta K$  becomes very small and the corresponding terms can no longer be considered as dominant. On the contrary, only grid points with  $Ri$  close to neutral should be corrected. A more correct behavior of the AFS should then be to act similarly as the original one for points close to neutrality, and that the grid points with  $Ri > 1$  should be just slightly corrected or even not.

#### 4.1. Proposed schemes

The key idea for the new AFS in ARPÈGE/ALADIN is still to constrain the numerical growth rate for each point, in the same spirit as in GD90. Unfortunately, this can no longer be done by directly inverting the numerical stability equation for  $\beta$ , in our practical case, because the expressions for dynamical and thermal exchange coefficients are no longer identical (as they were in GD90), and this leads to a more complex stability equation. Considering the unsuccessfulness of neglecting some terms as done in the original

AFS in ARPÈGE/ALADIN, an indirect method for insuring stability from this equation must be found.

For a given  $\beta$  or  $\tau$ , the function  $F(\beta, \tau)$  in (12) is a parabola. For  $\beta = 1$  the function  $F(1, \tau)$  has a minimum. The roots are the following:

$$\tau_{1,2}(1) = 0.5\{-B(1) \pm [B(1)^2 - 4A(1)C(1)]^{0.5}\}/A(1) \quad (14)$$

Both  $\tau_1(1)$  and  $\tau_2(1)$  are generally real, and then negative. It can happen (but very rarely, in about 1% of all grid points in our experiments) that  $\tau_1(1)$  and  $\tau_2(1)$  are complex-conjugate with negative real part, and a very small imaginary part. In this case the stability condition for the module of the numerical amplification factor  $x$  is:

$$|x| = [(1 + \tau_{\text{real}}(1))^2 + (\tau_{\text{imag}}(1))^2]^{0.5} < \varepsilon - 1 \quad (15)$$

where:

$$\tau_{\text{real}}(1) = -0.5 B(1)/A(1) \quad (16a)$$

$$\tau_{\text{imag}}(1) = \pm 0.5 [4 A(1) C(1) - B(1)^2]^{0.5}/A(1) \quad (16b)$$

represent the real and the imaginary parts of the roots. It can be shown that these few points with complex roots are not a source of fibrillations in ARPÈGE/ALADIN, and can conveniently be ignored for designing the AFS: according to our experience, this happens for grid-points with Richardson number near to neutral ( $0 < Ri < 0.5$ ) and atypically low values of turbulent exchange coefficients. The analysis shows that under these special conditions required for complex roots, the stability criterion is necessarily fulfilled, justifying the legitimacy of ignoring any AFS correction in these cases (Appendix B).

If  $\tau_1(1)$  and  $\tau_2(1)$  are real negative, the growth rate  $x$  associated with the smaller one (*i.e.* which has the largest magnitude, *e.g.*  $\tau_1(1)$ ) is given by:  $x = 1 - \tau_1(1)$ . The new scheme then consists in locally imposing  $\beta$  in such a way that the numerical growth rate  $x$  remains under a threshold value ( $\varepsilon - 1$ ) with  $\varepsilon \in [1, 2]$ . This new parameter specifying the maximum tolerated numerical growth-rate is basically the degree of freedom, which will allow the tuning of the scheme. If  $\tau_1(1) > -\varepsilon$ , fibrillations will be spontaneously damped by the factor  $(\varepsilon - 1)$  and thus no correction is necessary. The grid point is then said to be »stable«. Otherwise, a new bigger  $\beta$  has to be found which will satisfy the requested condition  $\tau(\beta) > -\varepsilon$  and this grid point will then said to be »unstable«. One has to rewrite the equation (8) in  $\beta$ , where  $\tau$  which is now fixed to  $-\varepsilon$ :

$$F(\beta, \varepsilon) = \beta^2 A'(\varepsilon) + \beta B'(\varepsilon) + C'(\varepsilon) = 0 \quad (17)$$

The new  $\varepsilon$ -dependent coefficients are defined by:

$$A'(\varepsilon) = \varepsilon\gamma^2 K_u K_\Theta$$

$$B'(\varepsilon) = \varepsilon^2 (\gamma K_u + \gamma K_\Theta) - \varepsilon\gamma^2 K_u K_\Theta (3 - 2\alpha_u + \alpha_\Theta)$$

$$C'(\varepsilon) = \varepsilon^2 - \varepsilon[\gamma K_\Theta (1 + \alpha_\Theta) - 2\gamma K_u (1 - \alpha_u)] + \gamma^2 K_u K_\Theta (2 - 3\alpha_u + \alpha_\Theta)$$

The obtained equation is still a parabola for a given  $\varepsilon$ . Since  $A'(\varepsilon)$  is positive and  $F(1, \varepsilon) < 0$ , this equation has two real roots, one of them being larger than 1. Choosing this root for  $\beta$  guarantees the stability of the scheme.

For our study of the impact of the corrections, three formulations are now examined:

1) over-simplified formulation:  $\beta$  is set to some constant value for all grid points and time-steps;

2) simplified formulation:  $\beta$  is set to some constant value for all grid points that need to be corrected;

3) exact formulation: the exactly obtained value of  $\beta$  is set for grid points that need to be corrected.

Using the third one, the integration will be more accurate, but more expensive because an exact computation of  $\beta$  has to be done for each unstable point. The second one would be cheaper in CPU-time usage, but in counterpart, less accurate. The first one is used for estimating the order of magnitude of the impact of the decentering factor in an absolute way.

#### 4.2. Results with new anti-fibrillation schemes

##### 4.2.1. $\beta = \text{const.}$

Preliminary testing with constant value  $\beta$  for every point and every time-step during the integration was done to obtain the estimation of what order should be the correction in the scheme to avoid fibrillations. According to the results (not shown here)  $\beta$  taken between 1.2 and 1.5 should be enough to damp the fibrillations. But this oversimplified version of the scheme is not usable since it is not at all accurate enough.

##### 4.2.2. Simplified formulation

It was a natural conclusion that there is no need to act on all grid points but only where the scheme is unstable. The simplest way is to use  $\beta = 1$  where scheme is stable and some constant value where it is not. The tests with  $\beta = \text{const.}$  everywhere showed that reasonable value would be 1.2–1.5. But, the choice of  $\beta$  for such step-function depends on damping factor  $x$ , *i.e.*  $\varepsilon$ . It determines the maximum  $\beta$  value that would be obtained during one run. Figure 5 shows the integration curves for the low-level temperature for  $\beta = 1.2$  and 1.5 respectively, and for  $\varepsilon = 1.75$ . The results show the absence of fibrillations from the latest period of integration, but also the appearance of some oscilla-

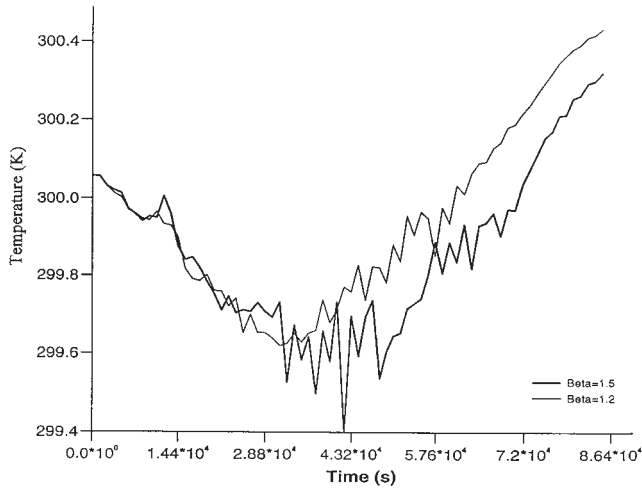


**Figure 5.** Evaluations of temperature during 24 hours time integration on level 26 in 1-D version of ARPÈGE model (new AFS,  $\Delta t = 1200$ s) with one constant value of  $\beta$  (step correction function) used always when  $\tau < -1.75$ ;  $\beta = 1.2$  (thin) and  $\beta = 1.5$  (thick).

tions in the middle part of the integration. Since  $\beta$  was chosen arbitrarily, maybe over- maybe underestimating the necessary value for damping fibrillations, the evolution was less accurate.

#### 4.2.3. Exact formulation

Figure 6 shows all (optimal)  $\beta$  values for »unstable« grid points obtained by the new scheme for various  $\varepsilon$  between 1 and 2. It can be seen that maximum  $\beta$  for each given  $\varepsilon$  decreases hyperbolically by the increase of  $\varepsilon$ . This

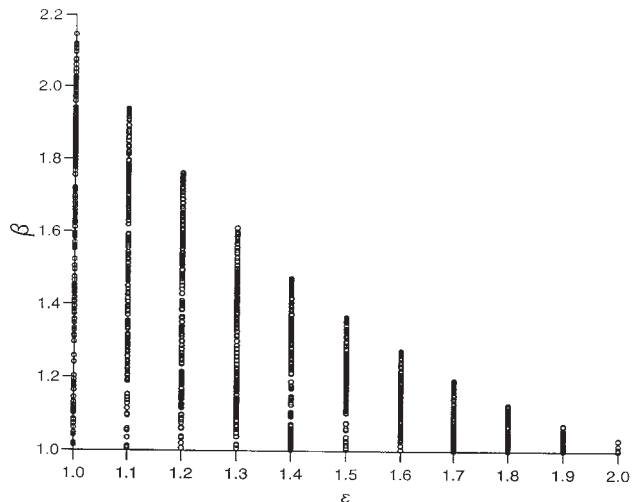


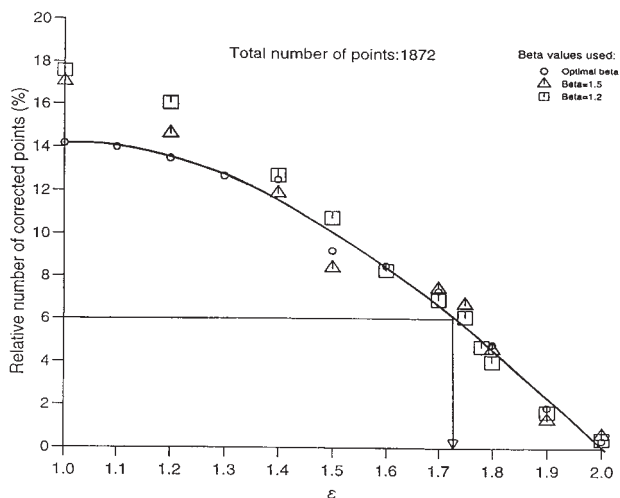
**Figure 6.**  $\beta$  values obtained by the new AFS during 24 h evaluation for »unstable« grid points for different values of damping factor  $\varepsilon$  ( $\Delta t = 1200$ s).



could be useful if one wants to act on »unstable« grid points by only one value for  $\beta$  (step correction function). In that case one should put the maximal possible  $\beta$  for chosen  $\varepsilon$  to be sure that all »unstable« grid points will be corrected to satisfy  $|x| < \varepsilon - 1$ .

Also, it is important to lessen the number of corrected grid points from almost 90% in the operational AFS to some more reasonable value (5% or so). Figure 7 shows the relative number of corrected grid-points as a function of the tuning parameter  $\varepsilon$  in three different cases ( $\beta = 1.2$ ,  $\beta = 1.5$  as in the previous section, and optimal local value). First, the proportion of corrected points is relatively insensitive to the exact value of  $\beta$  at least for  $\varepsilon$  close to 2. For smaller values, simplified schemes tend to generate more »unstable« points during the integration. Second, for the exact scheme, the proportion of corrected points shows a regular decreasing variation with respect to  $\varepsilon$  and can be fitted by a polynomial, which allows to tune the scheme in terms of this proportion of corrected points. For instance, the arrow shows the value of  $\varepsilon$ , to be chosen to correct only 6% of all points during the integration.

**Figure. 7.** Relative number of »unstable« grid points during 24 h evaluation ( $\Delta t = 1200$ s) when step correction function ( $\beta = 1.2$  (squares) and  $\beta = 1.5$  (triangles)) and  $\beta$  obtained by the new AFS (circles) was used for different values of damping factor,  $\varepsilon$ . Drawing the best-fit curve one can determine the approximate relative number of corrected grid points for the damping factor of interest.



Results obtained by the new scheme and by choosing the optimal value of  $\beta$  everywhere show a significant improvement in comparison with the operational one. Figure 8a shows the resulting temperature and curves on the 26th layer for three different values of  $\varepsilon$  (2, 1.75, 1.5) for 1200 s and Figure 8b for 600 s time-steps. Decreasing  $\varepsilon$  from 2 towards 1, the amplitude of fibrillations starts to decrease as well. For  $\varepsilon = 1.75$  most of the oscillations due to fibrillations are successfully removed. In that case (according to Figure 7) the scheme was acting only approximately 5% of all data. As mentioned above,

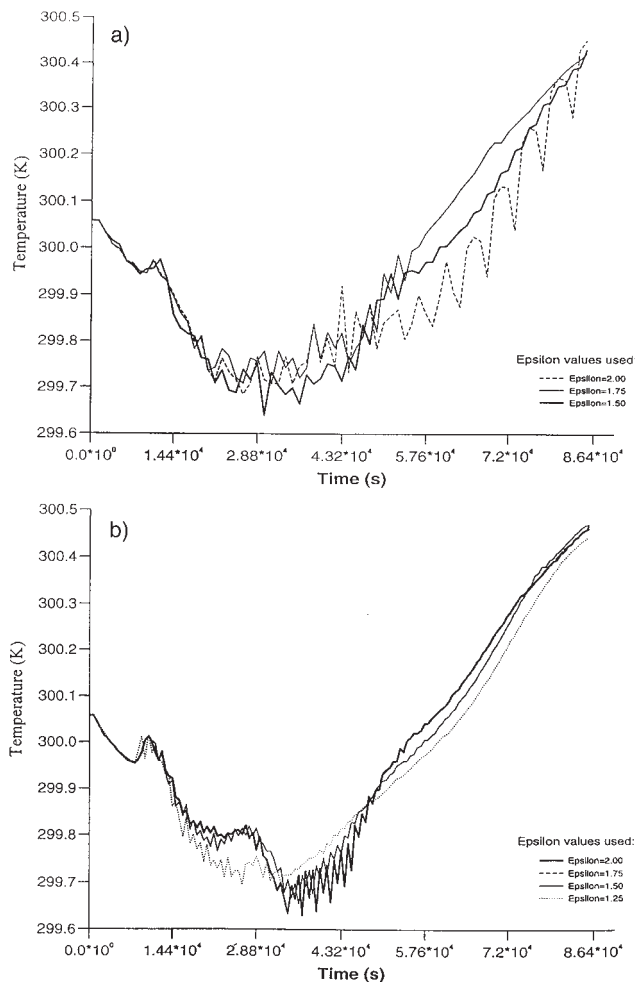


**Figure 8.** Evaluation of temperature during 24 hours time integration on level 26 in 1-D version of ARPÈGE model, a) ( $\Delta t = 1200\text{s}$ ) with different values of the damping factor:  $\varepsilon = 2.0$  (dashed),  $\varepsilon = 1.75$  (solid) and  $\varepsilon = 1.5$  (thick solid), and b) ( $\Delta t = 600\text{s}$ ), damping factor:  $\varepsilon = 2.0$  (thick solid),  $\varepsilon = 1.75$  (dashed),  $\varepsilon = 1.5$  (solid) and  $\varepsilon = 1.25$  (dotted).

the irregular oscillations in the first half of the integration are not due to the fibrillation process by itself and should not be expected to disappear by applying the AFS.

Figure 9 shows the optimal  $\beta$  values as a function of  $Ri$  plotted for different values of damping parameter  $\varepsilon$ . A major difference between the new AFS and both the operational one and that one proposed by and GD90 is that the new one implies a correction to grid points for which  $Ri < 0$ . When increasing the tuning parameter  $\varepsilon$  from 1 toward 2, the number of atmospheric unstable grid points to be corrected naturally decreases, and a smaller part of the atmospheric unstable domain is concerned, until finally for  $\varepsilon = 2$  only very few of this grid points should be corrected, and all in the atmospheric stable do-

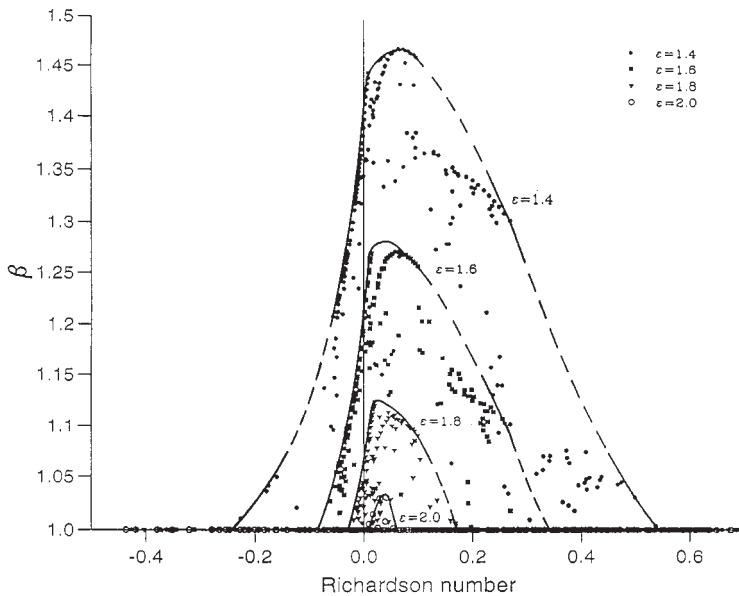


**Figure 9.**  $\beta$  values (obtained by the new AFS during 24 h evaluation,  $\Delta t = 1200s$ ) versus  $Ri$  for different values of damping parameter:  $\varepsilon = 2.0$  (circle),  $\varepsilon = 1.8$  (solid triangle),  $\varepsilon = 1.6$  (solid square) and  $\varepsilon = 1.4$  (solid circle).

main. The interval of Richardson numbers for which  $\beta = 1$ , is not always enough to prevent fibrillation that decreases when  $\varepsilon$  increases. The last striking feature is that a great majority of points, even in the moderate  $Ri$  domain do not need any correction, opposite to the operational AFS which corrected all moderate  $Ri$  points, and thus led to a significant loss of accuracy.

Comparing Figures 4 and 9 one can ask what is the reason why the new AFS is much more stable while much less correction is applied globally. This could be seen as a paradox: in the new AFS the width of the  $Ri$  interval where grid points are corrected is much narrower, and even in this interval, there is a large majority of not corrected grid points, but the resulting scheme is more stable. The clue is immediately suggested by comparing Figures 4 and 9 the small part of corrected points in the small  $Ri < 0$  region plays a very important role in the development of the instability in our case (which, once more, is more general as GD90's one). To prove this assertion, a test was made with neglecting to correct »unstable« grid-points in the domain  $Ri < 0$  with the new scheme. Figures 10a, b show the curves of integration (temperature and zonal wind component on the 26th layer) for  $\beta$  always set to 1 (*i.e.* no AFS at all) and with the optimal  $\beta$  obtained by the new scheme but applied only if  $Ri > 0$  ( $\beta = 1$  else). The damping parameter  $\varepsilon$  was chosen to

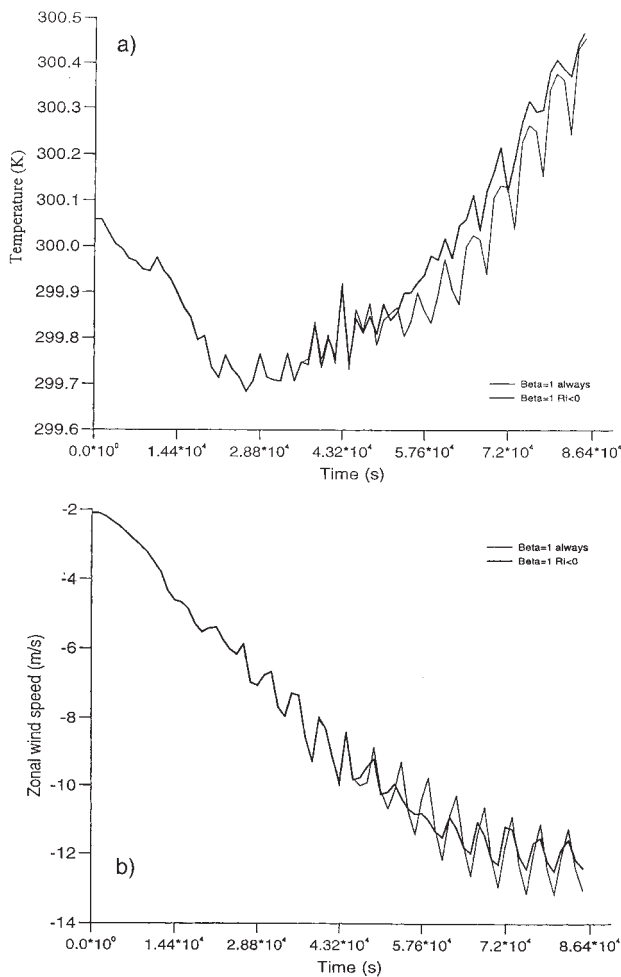


**Figure 10.** a) Evaluation of temperature during 24 hours time integration on level 26 in 1-D version of ARPÈGE ( $\Delta t = 1200$ s) with  $\beta = 1$  always (thin) and the new scheme but with  $\beta = 1$  for  $Ri < 0$  (thick). Damping factor is:  $\varepsilon = 1.75$ , b) The same for zonal wind component,  $u$ .

1.75. Neglecting the correction for  $Ri < 0$  causes the evolution to be similar to the one with no correction applied. According to this result it is clear that in the more general case where the dynamical and thermal exchange coefficients are not equal, the atmospheric unstable part of the flow can play a major role in the development of the vertical diffusion scheme's instability.

## 5. Conclusions

We investigated here the problems leading to time-instabilities in the current physics package of ARPÈGE NWP model. The occurrence of these instabilities appears to be the limiting factor for enlarging the time-step in the

current operational version. In the first part, the shallow convection correction (*CSC*) is identified as a major source of temporal oscillations, and some simple modifications are proposed to eliminate the intermittence of the scheme bearing in mind that solving definitely the problem would probably need to use a separate, more sophisticated parameterization scheme for this particular process. In the second part, another source of oscillations is shown to find its source in the vertical diffusion scheme, in spite of the application of a correction scheme directly based on Girard and Delage (1990) proposal.

This study shows that:

- Fibrillations occur with the operational scheme already with time-steps of 600 s and that their amplitude increase with increasing time-step.

- Operational scheme acts on a very large number of grid points (but only with positive  $Ri$ ) up to  $\beta_{\max} \approx 1.2$ .

- Using a less restrictive stability analysis, a new scheme can be derived, with a degree of freedom based on the maximum tolerated numerical growth rate, and taking the optimal  $\beta$  parameter for correction at each grid point.

- Some points lead to complex numerical growth rate, but with a real part too small to trigger instability. These points are currently ignored by the new AFS, apparently with no detrimental impact.

- A stable and more accurate integration evolution can be obtained since the scheme is more selective: it acts only on small number of grid points (typically 5%).

- Neglecting the correction for negative  $Ri$  only leads to a partial damping of the fibrillations, and this phenomenon is expected to appear as soon as the dynamical and thermal exchange coefficients are different.

Considering these results, the implementation of the new anti-fibrillation scheme could be of big practical importance, since the operational time-step could then be significantly increased while the integrations could even exhibit less oscillations.

*Acknowledgments* – The authors are greatly indebted to J.-F. Geleyn and J.-M. Piriou for their invaluable advice and assistance during many phases of this work. M. T. P. and A. M. were supported by RC-LACE and the French Ministry of Foreign Affairs while working at CNRM/GMAP at Météo-France.

## References

- ALADIN International Team, (1997): The ALADIN Project: Mesoscale modelling seen as a basic tool for weather forecasting and atmospheric research, WMO Bulletin, **46** (4), 1997, 317–324.
- Bubnová, R., A. Horányi and S. Malardel (1993): International project ARPÈGE/ALADIN. EW-GLAM Newsletter, **22**, 117–130.

- Courtier, Ph., C. Freyrier, J.-F. Geleyn, F. Rabier and M. Rochas (1991): The ARPÈGE project at Météo-France. ECMWF 1991 Seminar Proceedings: Numerical methods in atmospheric models, ECMWF, Reading, United Kingdom, 193–231.
- Haltiner, G. J. and R. T. Williams (1980): Numerical prediction and dynamical meteorology. John Wiley and Sons, New York, 477 pp.
- Geleyn, J.-F. (1987): Use of a modified Richardson number for parameterizing the effect of shallow convection. Collection of papers presented at the WMO/IUGG NWP Symposium, Tokyo, 4–8 August 1986, 141–149.
- Girard, C. and Y. Delage (1990): Stable schemes for nonlinear vertical diffusion in atmospheric circulation model. *Mon. Wea. Rev.*, **118**, 737–745.
- Kalnay, E. and M. Kanamitsu (1988): Time schemes for strongly nonlinear damping equations. *Mon. Wea. Rev.*, **116**, 1945–1958.
- Simmons, A. J. and D. M. Burridge (1981): An energy and angular-momentum conserving vertical finite-difference scheme and hybrid vertical coordinates. *Mon. Wea. Rev.*, **109**, 758–766.

## Appendix A

The coupled system represented by Eqs. (6) and (7) discretized in time with anti-fibrillation scheme becomes (Courtier et al., 1991):

$$\frac{\Psi^+ - \Psi}{\Delta t} = \left[ (1 - \beta)K_\Psi \Psi_z + \beta(K_\Psi \Psi_z^+) \right]_z, \quad (\text{A1})$$

and after rearranging:

$$\left[ 1 - \Delta t \frac{\partial}{\partial z} \left( \beta K_\Psi \frac{\partial}{\partial z} \right) \right] \left( \frac{\Psi^+ - \Psi}{\Delta t} \right) = (K_\Psi \Psi_z)_z, \quad (\text{A2})$$

where  $\Psi$  denotes  $u$  or  $\Theta$ , and  $[\ ]_z = \partial/\partial z$ . The right hand side (RHS) can be rewritten as:

$$(K_\Psi \Psi_z)_z = K_\Psi \Psi_{zz} + \frac{\partial K_\Psi}{\partial z} \Psi_z \quad (\text{A3})$$

where  $K_u$ ,  $K_\Theta$  and  $Ri$  are defined by Eqs. (3), (4) and (5).

Vertical derivative of the  $Ri$  is defined by:

$$\frac{\partial Ri}{\partial z} = Ri \left( \frac{\Theta_{zz}}{\Theta_z} - 2 \frac{u_{zz}}{u_z} \right). \quad (\text{A4})$$

Thus:

$$\frac{\partial K_\Psi}{\partial z} = K_\Psi \left[ (1 - 2\alpha_\Psi) \frac{u_{zz}}{u_z} + \alpha_\Psi \frac{\Theta_{zz}}{\Theta_z} \right] \quad (\text{A5})$$

where  $\alpha_u$  and  $\alpha_\Theta$  are defined by Eqs. (9) and (10).

Finally the coupled system becomes:

$$\left[1 - \Delta t \frac{\partial}{\partial z} \left( \beta K_u \frac{\partial}{\partial z} \right) \right] \left( \frac{u^+ - u}{\Delta t} \right) = K_u (2 - 2\alpha_u) u_{zz} + \frac{K_u \alpha_u}{\Lambda} \Theta_{zz} \quad (\text{A6})$$

$$\left[1 - \Delta t \frac{\partial}{\partial z} \left( \beta K_\Theta \frac{\partial}{\partial z} \right) \right] \left( \frac{\Theta^+ - \Theta}{\Delta t} \right) = K_\Theta (1 + \alpha_\Theta) \Theta_{zz} + K_\Theta \Lambda (1 - 2\alpha_\Theta) u_{zz} \quad (\text{A7})$$

where  $\Lambda = (\partial\Theta/\partial z)/(\partial u/\partial z)$ .

Linearization is made away a stationary state noted with bars. For the basic state to be stationary, it is required that both terms on the RHS are equal to zero in the basic state, which means that:

$$\frac{\partial \bar{u}}{\partial z} = \text{const.} \quad \text{and} \quad \frac{\partial \bar{\Theta}}{\partial z} = \text{const.}$$

and therefore

$$\frac{\partial \bar{K}}{\partial z} = \frac{\partial \bar{Ri}}{\partial z} = \frac{\partial \bar{\alpha}}{\partial z} = \frac{\partial \bar{\Lambda}}{\partial z} = 0.$$

The linearized form of the equations for the perturbations ( $u'$ ,  $\Theta'$ ) is the (bars are left out for clarity):

$$\left[1 - \Delta t \beta K_u \frac{\partial^2}{\partial z^2} \right] \left( \frac{u'^+ - u'}{\Delta t} \right) = K_u (2 - 2\alpha_u) u'_{zz} + \frac{K_u \alpha_u}{\Lambda} \Theta'_{zz} \quad (\text{A6})$$

$$\left[1 - \Delta t \beta K_\Theta \frac{\partial^2}{\partial z^2} \right] \left( \frac{\Theta'^+ - \Theta'}{\Delta t} \right) = K_\Theta (1 + \alpha_\Theta) \Theta'_{zz} + K_\Theta \Lambda (1 - 2\alpha_\Theta) u'_{zz} \quad (\text{A7})$$

Oscillating solutions are sought in the form:

$$u' = u_0 \exp(imz + \omega t)$$

$$\Theta' = \Theta_0 \exp(imz + \omega t)$$

where  $\omega$  is the growth rate. We assume the following discretized form for the vertical Laplacian operator:

$$\frac{\partial^2}{\partial z^2} X_l = \frac{X_{l+1} - 2X_l + X_{l-1}}{(\Delta z)^2}$$

and we note  $x = \exp(\omega \Delta t)$ . The coupled system then becomes:

$$\left[ (1 + \beta \gamma K_u)(x - 1) + \gamma K_u (2 - 2\alpha_u) \right] u' + \gamma \frac{K_u \alpha_u}{\Lambda} \Theta' = 0 \quad (\text{A8})$$

$$\gamma K_\Theta \Lambda (1 - 2\alpha_\Theta) u' + \left[ (1 + \beta \gamma K_\Theta)(x - 1) + \gamma K_\Theta (1 + \alpha_\Theta) \right] \Theta' = 0 \quad (\text{A9})$$

Eliminating the perturbations then give the characteristic equation (8) for  $\tau = x - 1$ :

$$\begin{aligned} & \tau^2[(1 + \beta\gamma K_u)(1 + \beta\gamma K_\ominus)] + \tau[(1 + \beta\gamma K_u)\gamma K_\ominus(1 + \alpha_\ominus) + (1 + \beta\gamma K_\ominus)\gamma K_u(2 - 2\alpha_u)] \\ & + [\gamma^2 K_u K_\ominus(2 - 3\alpha_u + 2\alpha_\ominus)] = 0 \end{aligned}$$

## Appendix B

Depending on the damping parameter  $\varepsilon$ , it is possible that the scheme with  $\beta = 1$  gives complex roots of Eq. (12) for very few grid points (about 1% of all). Their characteristics are:

- 1) slightly positive atmospheric stability ( $0 < Ri < 0.4 - 0.5$ ) and
- 2) small values for terms with exchange coefficients ( $\gamma K_u, \gamma K_\ominus$ ) of the order of  $10^{-2}$ .

To keep the scheme numerically stable, the module of the numerical amplification,  $x$ , has to satisfy the condition of stability given by Eq. (17). The condition can be simplified by putting  $\varepsilon = 2$ :

$$[(1 + \tau_{\text{real}})^2 + \tau_{\text{imag}}^2]^{0.5} < 1. \quad (\text{B1})$$

Inserting terms (16a), (16b) with a general value of  $\beta$  for coefficients  $A, B$  and  $C$ , the following relation is obtained after some algebra:

$$B(\beta) - C(\beta) > 0. \quad (\text{B2})$$

The goal is to find  $\beta$  which would satisfy (B2). Inserting terms for  $B(\beta)$  and  $C(\beta)$  and separating  $\beta$  the following relation is obtained:

$$\beta > \frac{2 - 3\alpha_u + 2\alpha_\ominus}{3 - 2\alpha_u + \alpha_\ominus} - \frac{\gamma K_\ominus(1 + \alpha_\ominus) + 2\gamma K_u(1 - \alpha_u)}{\gamma^2 K_u K_\ominus(3 - 2\alpha_u + \alpha_\ominus)} \quad (\text{B3})$$

In our particular case, the first term on the RHS of (B3) is always positive and of order  $10^{-1}$ . Because of  $\gamma^2 K_u K_\ominus \ll 1$  in the denominator, the second term becomes dominant and since its nominator is positive,  $\beta$  has to be greater then some negative number of the order of  $10^1 - 10^2$ , in order to fulfill the numerical stability condition. According to this,  $\beta = 1$  is sufficient for this purpose.



## SAŽETAK

**Poboljšanje sheme vertikalne difuzije u  
ARPÈGE/ALADIN modelu***Maja Telišman Prtenjak, Antun Marki i Pierre Bénard*

Učinkovite numeričko-dinamičke sheme u atmosferskim numeričkim prognostičkim modelima dozvoljavaju uporabu duljeg vremenskog koraka prilikom numeričke integracije, ali često dolazi do neželjenih oscilacija uzrokovanih parametrizacijom fizikalnog dijela. Tipičan primjer je pojava oscilacija povezanih s pojednostavljenim parametrizacijskim shemama za vertikalnu difuziju ili plitku konvekciju, koje se uobičajeno koriste u numeričkoj prognozi vremena.

Oscilacije koje se generiraju shemama vertikalne difuzije K-tipa do sada su detaljno razmatrane, i nazvane su *fibrilacijama*. Visoke prostorne i vremenske frekvencije karakteristike su fibrilacija. Zbog njihove povezanosti s velikom vertikalnom rezolucijom, ove lažne oscilacije se općenito uočavaju na nižim nivoima domene modela.

U prognostičkim poljima ARPÈGE-a (numeričkom prognostičkom globalom modelu u MÉTÉO-FRANCE) i ALADIN-a (njegovoj verziji modela za ograničeno područje razvijenom u suradnji sa zemljama istočne Europe) neke oscilacije su se i dalje zadržale unatoč činjenici da je uključena prva anti-fibrilacijska shema (AFS). Ovaj rad prikazuje provedena ispitivanja mogućih izvora fibrilacija pomoću 1-D (vertikalne) verzije ovih modela.

Ispitivanja su dala slijedeće rezultate: 1. znatan izvor oscilacija je pronađen u parametrizaciji plitke konvekcije (što je u stvari dio sheme vertikalne difuzije) te su predložena neka rješenja za njihovo uklanjanje, 2. pokazalo se da početna AFS ne može u potpunosti spriječiti generiranje fibrilacija te je izvedena uspješnija formulacija.

Jednadžbe vertikalne difuzije prikazane u numeričkom vremenskom raspisu prvog reda, zadržavajući eksplicitnu formu samog koeficijenta izmjene, u osnovi sadrže AFS. Stoga, korekcija AFS-om uvijek poboljšava stabilnost na račun točnosti. S novom anti-fibrilacijskom shemom, broj točaka mreže u kojima je potrebno izvršiti korekciju smanjen je s gotovo 90% na približno 5%, čime je shema dobila na točnosti. Za razliku od predloženih AFS iz literature, korekcija se mora primjenjivati ne samo na točke mreže sa stabilnim atmosferskim uvjetima (Richardsonov broj,  $Ri > 0$ ) već i na one točke u kojima je atmosfera blago nestabilna ( $Ri < 0$ ).

*Corresponding author's address:* Dr. Pierre Bénard, Groupe de Modélisation pour l'Assimilation et la Prévision, Centre National de Recherches Météorologiques, Météo-France, 42 Avenue Coriolis, F – 31057, Toulouse Cedex, France (E-mail: pierre.benard@meteo.fr).